

The activity of non-metallic boron-doped diamond electrodes with sub-micron scale heterogeneity and the role of the morphology of sp^2 impurities

Kristína Cinková^a, Christopher Batchelor-McAuley^b, Marián Marton^c, Marian Vojs^c, Ľubomír Švorc^a and Richard G. Compton^{b*}

^aInstitute of Analytical Chemistry, Faculty of Chemical and Food Technology, Slovak University of Technology in Bratislava, Radlinského 9, Bratislava, SK-812 37, Slovak Republic

^bDepartment of Chemistry, Physical & Theoretical Chemistry Laboratory, Oxford University, Oxford OX1 3QZ, United Kingdom

^cInstitute of Electronics and Photonics, Faculty of Electrical Engineering and Information Technology, Slovak University of Technology in Bratislava, Ilkovičova 3, Bratislava, SK-812 19, Slovak Republic

* Corresponding author. E-mail: richard.compton@chem.ox.ac.uk (Richard G.Compton)

Abstract

The electrochemical activity of low boron-doped diamond electrodes prepared by hot filament chemical vapour deposition with varying methane levels in a hydrogen source gas ratio is studied by cyclic voltammetry (CV), Raman spectroscopy and scanning electron microscopy (SEM). The electrochemical response of the electrodes is found to be inconsistent with the electrodes acting as semi-conducting interfaces i.e. no diode like behavior is observable. Hence, on the basis of the presence of sp^2 and other non-diamond carbon impurities present in the electrode, the electrochemical response is ascribed as being dominated by these low level impurities masking any response of the boron that may or may not be present. Importantly, near fully reversible voltammetry of the redox probe ruthenium (III) hexamine is recorded and with increasing CH_4/H_2 ratio used for the preparation, the CV showed the electro-reduction in aqueous solution is found to exhibit a significant decrease in the voltammetric peak-to-peak separation. This changed electrode response is attributed to the altered morphology and dimensions of the non-diamond and graphitic sp^2 impurities where the larger impurity domains serve to decrease the electrode resistivity.

1. Introduction

Synthetic diamond offers advantages over traditional electrode materials including wide potential windows, chemically inert surfaces, low background currents, claimed minimal propensity to adsorption processes and mechanical robustness for applications. In particular, boron-doped diamond (BDD) has attracted increasing interest as an electrode material for applications in electroanalysis [1-6].

Diamond thin film electrodes are mostly prepared by means of chemical vapour deposition (CVD). To impart conduction in diamond films, they are commonly doped during growth with an acceptor (boron) to obtain a p-type conductivity. Various dopant concentrations are achieved by controlling the boron source resulting in formation of polycrystalline diamond. Conditions applied in the preparation process influence the boron doping level, grain size, crystallographic orientation, morphological defects, nondiamond carbon content (sp^2 inclusion), conductivity and in this regard the electrochemical performance [7,8]. The material is considered to be metal-like for 10^{20} B atoms cm^{-3} , semiconducting for dopant densities of 10^{19} B atoms cm^{-3} and lower with an intermediate region characterized by hopping conduction [9]. Un-doped diamond films deposited by CVD are generally electrochemically insulating [10]. However, incorporated non-diamond carbon impurities can provide charge carriers and play a role not only as active sites for electron transfer but also as stronger adsorption sites. Consequently, the sp^2/sp^3 ratio is an important parameter in controlling the electrochemical properties of un-doped diamond electrodes [11].

Beyond the properties of the bulk material, the diamond surface structure and its termination (with either oxygen or hydrogen) is also an important factor in determining the diamond electrode properties. Pre-treatment can lead to an increase in the free carrier concentration, presenting a possible route to electrochemical activity improvement [8,12]. Moreover, the

electrochemical activity may vary across the diamond electrodes because of the heterogeneous nature of the surface [13]. Surface conductivity has been observed in the case of hydrogen terminated un-doped diamond films after exposure to air. It was shown that hydrogen is necessary, but is not a sufficient prerequisite for the surface conductivity and acceptors that generate the hole accumulation layer are provided by atmospheric adsorbates [14]. Hydrogen terminated un-doped CVD diamond shows an insulator-metal transition if immersed into redox-electrolyte solutions with chemical potentials below the valence-band maximum. Due to electron transfer from the valence band into empty states of the electrolyte, a highly conductive surface layer is generated. The charge transfer inducing surface conductivity requires relatively defect free diamond and complete surface hydrogen termination [15,16].

The redox processes of un-doped nanodiamond film have been extensively studied by Holt et al [17]. Cyclic voltammetry showed extremely sluggish kinetics for all redox couples studied. These results were explained by assuming conduction takes place through sp^2 (graphitic and defect sites). It was concluded that the non-diamond component of the film introduces impurity bands into the band gap and allows limited metallic type conductivity. However, due to the heterogeneity of the surface, the results may be attributed to a mixture of sites of metallic and semiconducting nature. Potential cycling in nitric acid presents an effective route for the complete removal of electrochemically active sp^2 carbon that is highly aggregated within grain boundaries from the electrode surface. The removal accompanies a loss of electrochemical activity to form completely inactive nanodiamond phases [18]. The conductivity occurring along graphitized grain boundaries may be observed after changing initially insulating polycrystalline diamond films into a conducting material by high-temperature annealing in vacuum at the temperature above 1825 K. In this way, the diamond-graphite films can be of interest in electrochemical applications [19].

As a result, understanding the physical, chemical and electronical properties of low doped diamond electrodes, their response in aqueous media as well as mechanism of electron exchange between the electrode surface and solution of redox species is of interest. In this paper, we present a study of redox processes using low boron-doped thin film diamond electrodes exhibiting *sub-micron* scale heterogeneity prepared by CVD with various CH₄/H₂ ratios. Attention is paid to exploring the effect of relative amounts of non-diamond carbon impurities in the electrodes as well as the crystallite grain size and the resulting influence on the voltammetry. It is demonstrated how even for these non-metallic low boron-doped ($< 10^{20}$ B atoms cm⁻³) diamond electrodes graphitic carbon impurities and the electrode morphology has a significant influence over the electrochemical response. Consequently, analysis of the electrochemical response of BDD solely in terms of the boron content is unlikely to yield any significant physical insight even for electrodes with larger (> 100 nm) grain sizes. The characterisation of film morphology was studied by scanning electron microscopy (SEM) and the film microstructure by Raman spectroscopy. Cyclic voltammetric studies were performed using Ru(NH₃)₆^{3+/2+} as a redox probe.

2. Experimental

2.1. Preparation of low boron-doped diamond electrodes

The double bias enhanced hot filament chemical vapour deposition (HFCVD) technique was employed for the fabrication of polycrystalline low boron-doped diamond (PCD) film electrodes on highly conductive (0.008–0.024 Ω cm) N (100) type silicon with a 2 μm thick SiO₂ layer (CVD, Oxford PlasmaLab 80). The parameters of growth process were as follows: a pressure of 3000 Pa and a temperature of 650 ± 20 °C. As a working gas, the 0.5%, 1% and 2% mixture of methane in hydrogen was used. Although no boron was used in the synthesis gas, trace amounts of boron will remain in the deposition chamber from previous film preparations. The quantity of residual boron in the electrodes used in this study has been

determined by Neutron depth profiling (NDP) and Hall constant measurement [20] to be of the order of 10^{19} atoms per cm^{-3} . NDP was used utilizing a strong nuclear reaction of $^{10}\text{B}(\text{n}, \alpha)^7\text{Li}$ with a high cross section (3837 b) with the detection limit of 10^{12} B atoms per cm^3 and 15 nm as the depth resolution of the technique. To enhance the diamond nucleation density, 40 min ultrasonic seeding of diamond nanoparticles (CAS No. 7782-40-3, Sigma-Aldrich) diluted in deionised water was applied. After a growth time of 2 h, the as grown diamond layer remained exposed to an H_2 plasma for additional 10 min. Using standard optical lithography (SUSS, MA6) and wet etching in BOE solution (6:1 volume ratio of 40% NH_4F in water to 49% HF in water), the active area of electrode was created in 400 nm SiO_2 (CVD, Oxford PlasmaLab 80). A connection of the electrode chip ($10 \times 3 \text{ mm}^2$) was performed by an Ag polymer paste (CB115, DuPont) to a printed circuit board support and subsequently passivated by a non-conducting paste (548X, DuPont). Active surface areas of electrodes are 0.352 mm^2 for 0.5% and 0.396 mm^2 for 2.0% CH_4/H_2 .

2.2 Apparatus

The morphology and structure of the low boron-doped diamond electrodes were characterized by scanning electron microscopy (SEM, JEOL JSM-7500F) and Raman spectroscopy (HORIBA JOBIN YVON LABRAM 300, He–Ne laser 632 nm). Cyclic voltammetric measurements were recorded using a computer-controlled $\mu\text{Autolab III}$ potentiostat (Metrohm Autolab B.V., The Netherlands) using a glass electrochemical cell (25 mL) in a Faraday cage controlled by the NOVA 1.10 software. A standard three-electrode configuration was used, employing a saturated calomel reference electrode, a platinum microdisc electrode as a counter electrode and a low boron-doped diamond electrode as a working electrode. Prior to use, the working electrode was rinsed with deionised water. The analysis of experimental data was carried out with OriginPro 8.5 software (OriginLab Ltd.).

Two dimensional simulations of voltammetry were performed using software written in house [21] to allow for mixed linear and convergent diffusion. All experiments were carried out in a thermostated water bath at a temperature of 25 ± 0.1 °C.

2.3 Chemical reagents

Hexaamminruthenium chloride ($\text{Ru}(\text{NH}_3)_6 \text{Cl}_3$) and potassium chloride (KCl) at the highest available grade (99.0%) were purchased from Aldrich (Gillingham, UK) and used as received without any further purification. All aqueous solutions were prepared daily at 25 °C using deionised water with a resistivity of not less than $18.2 \text{ M}\Omega \text{ cm}$ (25 °C, Millipore UHQ, Vivendi, U.K.) as the solvent and KCl (0.1 M) as the supporting electrolyte. Solutions were degassed with nitrogen prior to all experiments.

3. Results and Discussion

This section starts with the characterisation of the low boron-doped diamond electrodes via surface imaging and Raman spectroscopy. Second, electrochemical characterisation provides evidence for the significant electroactivity of the low boron-doped diamond electrodes towards the electro-reduction of ruthenium (III) hexamine redox probe in aqueous solution. Finally, the physical and electrochemical characterisation of the electrodes is reconciled, yielding insight into the importance of the *morphology* of sp^2 and non-diamond carbon impurities.

3.1 Physical characterisation of low boron-doped diamond electrodes

The characterisation of the electrode surface morphology was performed by scanning electron microscopy (SEM). Fig. 1 shows representative images of the electrodes grown with increasing CH_4/H_2 ratios by the HFCVD. All three electrode materials exhibit a

polycrystalline structure, however, notably as the methane percentage is increased in the synthesis, the average grain size is found to increase as well. The average grain sizes are as follows: 140 nm for 0.5%, 280 nm for 1% and 490 nm for 2%. Hence in all cases the electrode surfaces comprise of sub-micron scale diamond crystals.

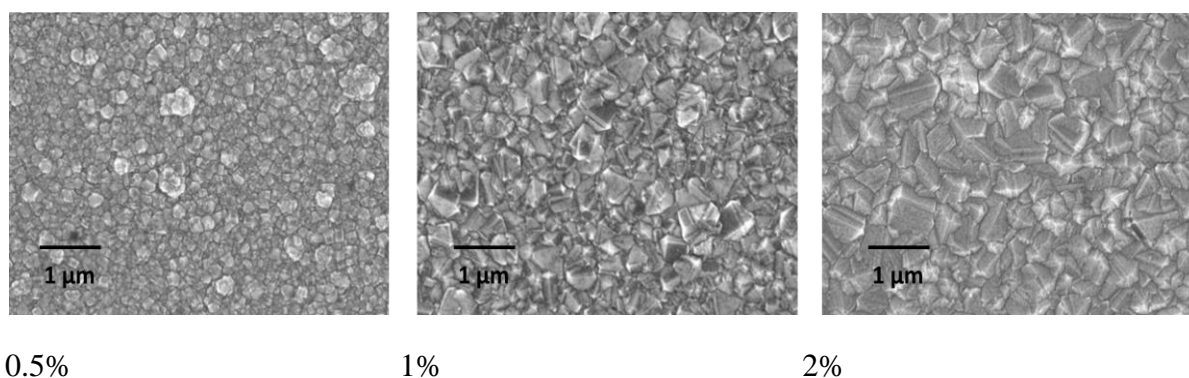


Fig. 1: SEM images of low boron-doped diamond films with various CH_4/H_2 ratios.

Further characterisation of the diamond film was undertaken using Raman spectroscopy, for which the raw data is shown in the Supporting information (SI) section 1. The Raman spectra were recorded using a wavelength of 632 nm and yield qualitative insight into the electrode microstructure and bonding. Apart from the Si and SiO_2 substrate peaks observable at 521 cm^{-1} and 950 cm^{-1} , three important features can be seen in the spectra. First, a peak at 1332 cm^{-1} corresponds to polycrystalline diamond (Di peak), second, a peak at approximately 1580 cm^{-1} (G peak) is a result of stretching of sp^2 bonds and third the bands at 1100 cm^{-1} and 1450 cm^{-1} , best visible for the 0.5 and 1% CH_4/H_2 ratios, are associated with isolated transpolyacetylene (TPA) sites at grain boundaries [22,23]. Analysis of the intensities and widths of these features yields insight into the structure and bonding.

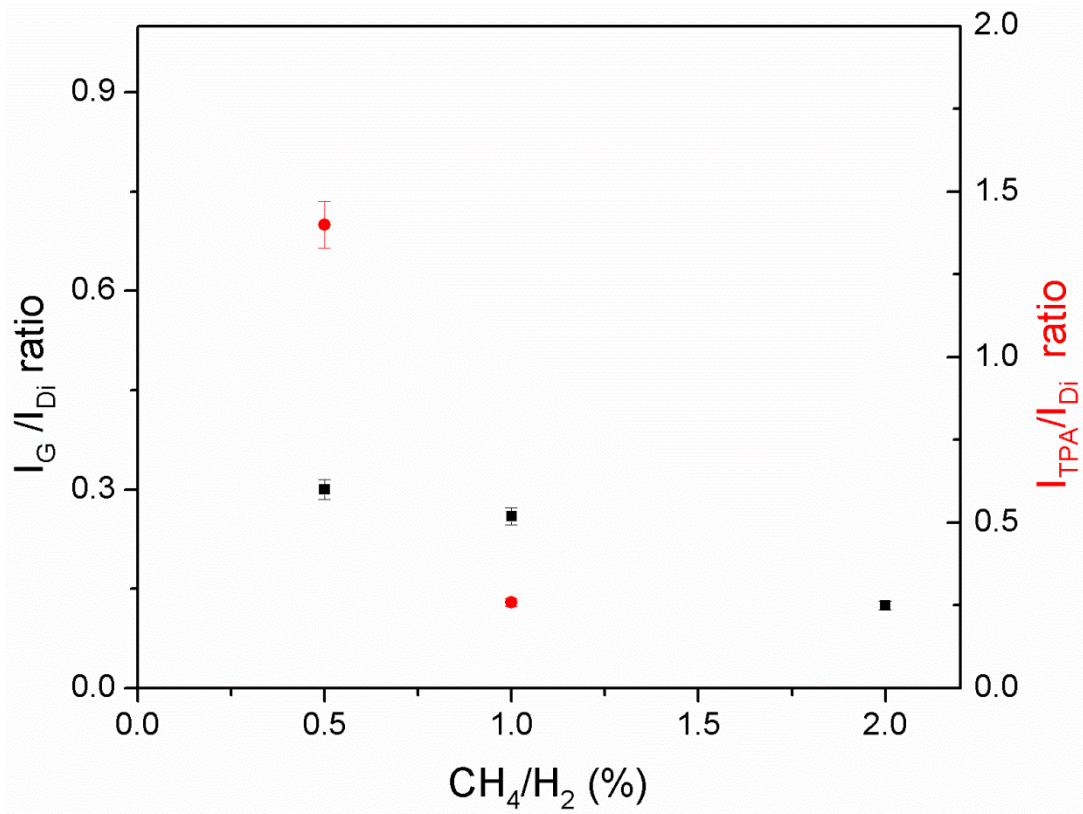


Fig. 2: Raman spectra I_G/I_{Di} and I_{TPA}/I_{Di} ratio as a function of CH_4/H_2 used in the synthesis.

Fig. 2 depicts the ratios of the graphite and transpolyacetylene peaks versus the diamond peak. Broadly, with increasing methane amount, the relative quantity of the sp^2 and transpolyacetylene impurities in the material decrease. A clearly defined transpolyacetylene peak is only observed for the lower CH_4/H_2 ratio. This is a commonly observed behaviour for increasing diamond crystal size and quality, because the sp^2 and trans-(CH_x) sites located mainly at grain boundaries, intra-grain dislocations and intergranular amorphous or graphitic regions. The relative increase of graphitic content can lead to a better electrical conductivity due to higher amount of conductive pathways and can be responsible for a larger number of surface active sites as well. On the other hand, lower crystal quality can influence the electrode stability and durability, especially in the case of ultrananocrystalline diamond thin films. From the ratio of magnitude of the Di and G peaks the qualitative information about the

sp^2 and sp^3 bonded carbon on the electrode surface can be estimated. Beyond analysis of the relative magnitudes of the Raman spectral peaks information can also be obtained through consideration of the peak widths, where for the amorphous carbon, the D and G peak widths are generally broader (the mixture of sp^3 and sp^2 carbon bonding) [9,22]. Hence, the broadness of the recorded Raman G peak predominantly reflects the locally amorphous character of the carbon surface.

3.2 Electrochemical characterisation

Given the low boron doping, i.e. below the metallic threshold, of the electrodes and the presence of sp^2 bonded carbon, one might anticipate that they would exhibit little electrochemical activity or may in accordance with the literature be observed to act as an electrochemical diode [24]. However, as will be demonstrated herein this is found to not be the case. In order to minimise the influence of specific adsorption and the influence of the surface morphology, ruthenium(III) hexamine ($Ru(NH_3)_6^{3+/2+}$) was used as an exemplar outer-sphere redox probe. The voltammetric response of the 0.5% CH_4/H_2 ratio diamond electrode was studied voltammetrically in a solution containing 0.1 – 3.0 mM $Ru(NH_3)_6^{3+/2+}$ (containing 0.1M KCl as supporting electrolyte) at a range of scan rates from 20 to 320 $mV\ s^{-1}$. The cyclic voltammetric scans were started at 0.2 V and initially scanned cathodically to -0.6 V (vs. SCE), the results of which are depicted in Fig. 3. For all ruthenium(III) concentrations experimentally used, a reductive voltammetric redox wave is exhibited and centred around the formal potential of the redox couple (in this work at -0.17 V vs. SCE in 0.1 M KCl). Respective experimental peak currents obtained for the forward scan by CV were compared to maximum peak currents calculated by the Randles-Ševčík equation [25] for the best electron transfer limit (so-called 'reversible' case):

$$I_p = 2.69 \times 10^5 n^{3/2} A D^{1/2} c \nu^{1/2} \quad (1)$$

where I_p = peak current (A), n = number of electrons, A = electrode area (cm^2), D = diffusion coefficient of ruthenium(III) hexamine ($\text{cm}^2 \text{s}^{-1}$), c = concentration (mol cm^{-3}) and ν = scan rate (V s^{-1}).

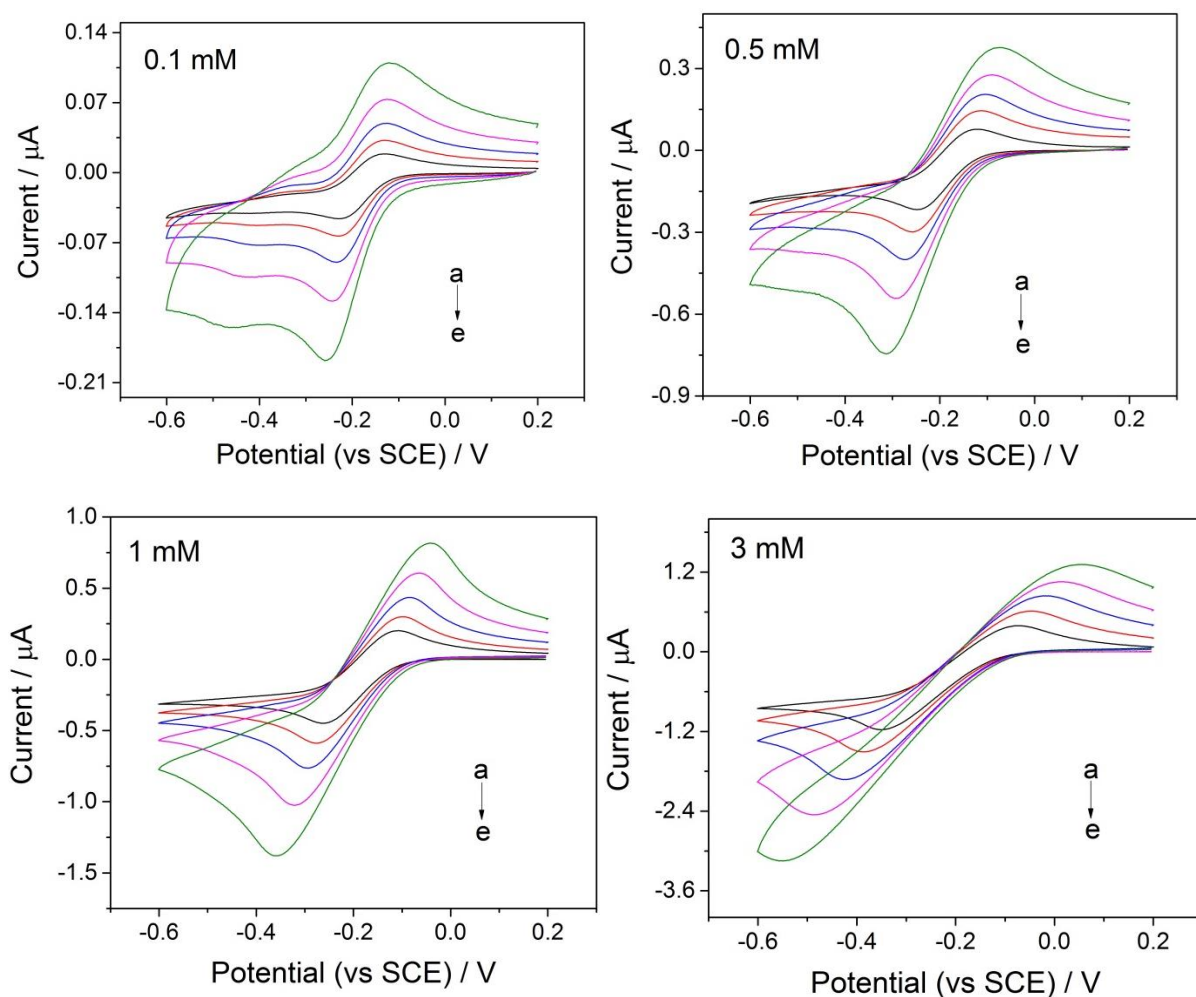


Fig. 3: Cyclic voltammetric responses of $\text{Ru}(\text{NH}_3)_6^{3+/2+}$ (0.1 – 3 mM) using a sub-micron scale thin-film electrode with a 0.5 % CH_4/H_2 ratio used in the synthesis. Scan rates: (a) 20, (b) 40, (c) 80, (d) 160, (e) 320 mV s^{-1} .

The voltammetric peak heights recorded for the lower concentrations of ruthenium(III) are in reasonable agreement with that predicted by the Randles-Ševčík equation using $D = 8.4 \times 10^{-6} \text{ cm}^2 \text{s}^{-1}$ (Fig. 4). For example, the calculated peaks heights are only 11.8%, 5.1% and 4.4% lower than experimental peak heights for the scan rates of 20, 80 and 320 mV s^{-1} . However,

at higher concentrations the peak currents deviate from the theoretical prediction, it will be discussed below that this discrepancy reflects the change in the voltammetric waveshape.

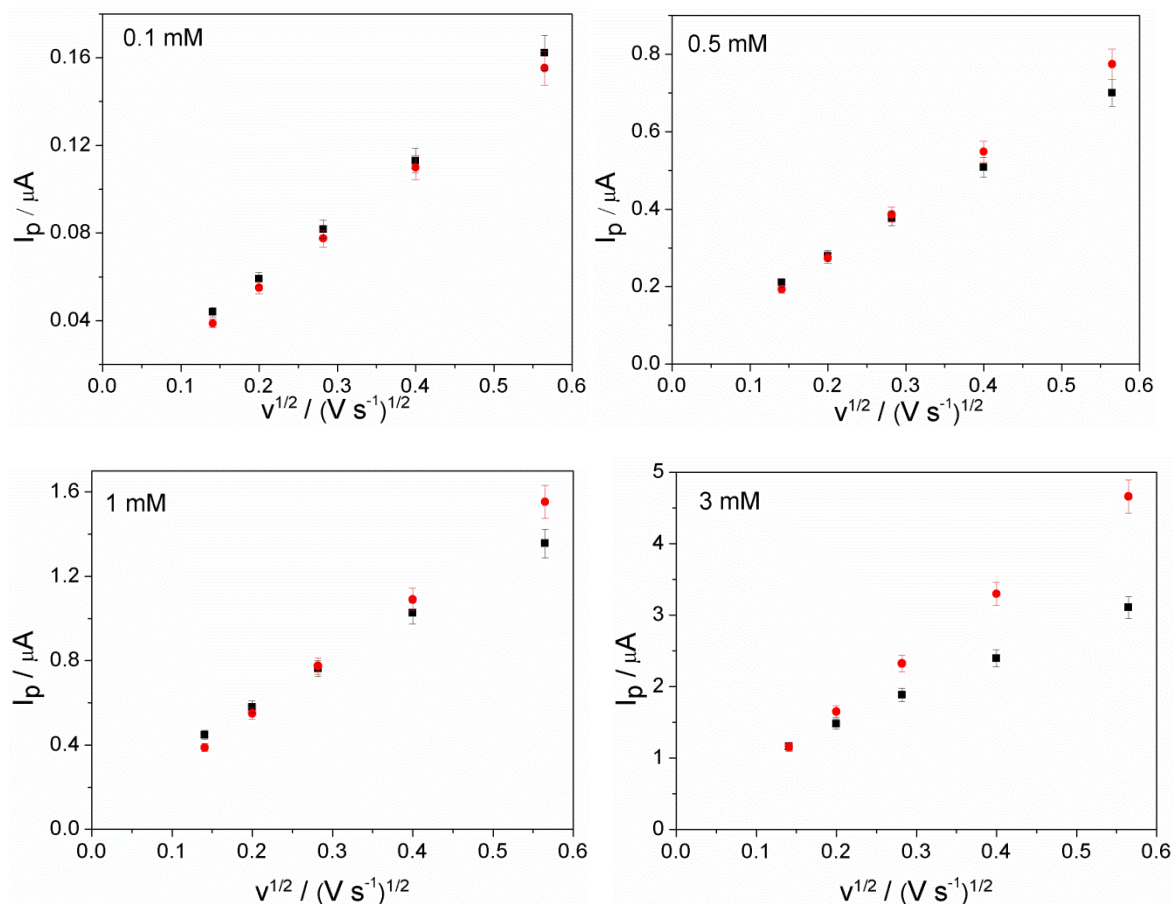


Fig. 4: Peak current (I_p) as a function of square root of scan rate ($v^{1/2}$) using electrode with 0.5% CH_4/H_2 ratio for various $\text{Ru}(\text{NH}_3)_6^{3+/2+}$ concentrations, black data - experimental, red data - calculated according to Randles-Ševčík equation.

Fig. 3 shows how the voltammetric waveshape recorded for the redox response of the $\text{Ru}(\text{NH}_3)_6^{3+/2+}$ couple at the 0.5% CH_4/H_2 diamond electrode varies as a function of the ruthenium(III) concentration in the range of 0.1 - 3 mM. The second broad wave appearing at the lowest concentration (0.1 mM) is tentatively ascribed as relating to the electrostatic adsorption of positively charged redox probe to the surface at these negative potentials. The voltammetric peak-to-peak separation increases as a function of scan rate and is, in all cases, greater than value

of ~57 mV typical for an electrochemically reversible couple, as shown in the SI section 2. Given the concentration of supporting electrolyte used within this work (0.1 M KCl), ohmic distortion due to a potential drop in the solution phase is not feasible [26]. The changed voltammetry might possibly relate to the altered reactivity of the electrode surfaces, however, due to the fast electron transfer kinetics associated with the $\text{Ru}(\text{NH}_3)_6^{3+/2+}$ redox couple it is more likely that the altered voltammetry arises due to resistance effects. The variation of the voltammetric waveshape as a function of the analyte concentration and as a function of the scan rate strongly indicates that the electrodes themselves are significantly resistive leading to the distorted voltammetric waveshape and subsequent suppression of the peak-heights, as compared to the Randles-Ševčík equation at high scan rates and high analyte concentrations. The close agreement, at low concentrations, of the peak current with the theoretically predicted value based upon the geometric area of the electrode strongly indicates that – although the surface is highly heterogeneous at the sub-diffusional scale i.e. below 10s of microns – the entire electrode surface is evidenced from the voltammetric response to be effectively active. To restate this point, even given the likely highly variable electroactivity of the surface the spacing between adjacent ‘active’ sites on the electrode must be less than the distance diffused by the ruthenium hexamine on the timescale of the voltammetric experiment. The types of the voltammetric behaviour for a heterogeneous electrode [27] are depicted in Fig. 5. In summary, case 1 is based on macroscopically large blocked and unblocked surface. The unblocked electrode experiences linear diffusion with unchanged concentration of electroactive species in vicinity of the electrode. However, the current scale of observed voltammogram is reduced. In case 2, micro-sized electroactive zones are separated and the electrode behaves as a collection of isolated microelectrodes with convergent diffusion. In the present case, the diffusion regimes associated with local active areas is a limiting situation of case 3, where the diffusion field of electroactive zones overlap

so strongly, such that, the diffusion regime to the *entire* electrode is effectively linear (the maximum distance between sites are estimated to be 65 - 260 μm via the Einstein equation $d \sim (2Dt)^{0.5}$) and heterogeneous electrode behaves like an unblocked electrode (Fig. 5, case 4) [27,28].

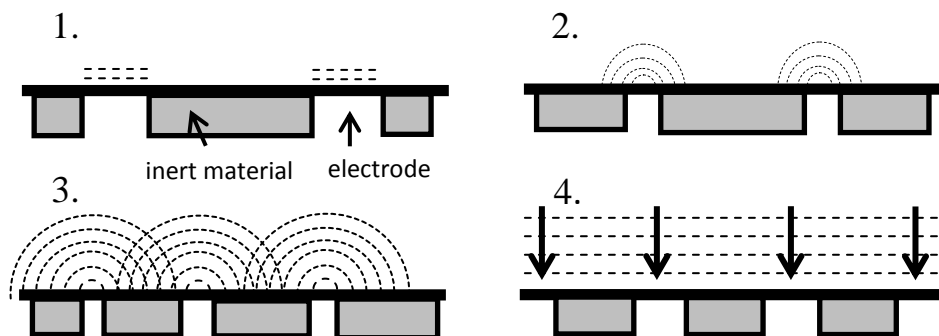


Fig. 5: Voltammetric behaviour for a heterogeneous electrode with active and inert zones illustrating the cases 1,2,3 and 4 discussed in the text.

As a consequence of this discussed possibility of diffusional overlap, a recorded electrochemical response may be totally dominated by a minority of active sites on an electrode surface. Any information regarding electron transfer to/from areas of lower activity – even if the surface coverage of the less active material is significantly greater – is therefore masked by the faster process occurring at the more active site.

Having electrochemically characterised the response of the 0.5% CH_4/H_2 diamond electrode towards the redox probe analogous voltammetric data was recorded for the 2% CH_4/H_2 diamond electrode. The full set of electrochemical characterisation data is shown in the SI section 3. Comparable results were obtained for the 2% CH_4/H_2 diamond electrodes where the peak current is in good agreement with the value of peak current predicted from the Randles-Ševčík equation. In order to aid direct comparison of the voltammetry recorded on the two electrodes, Fig. 6 shows the voltammetric responses of the 0.5 and 2% CH_4/H_2

electrodes towards variable concentrations (0.1 – 3 mM) of the ruthenium(III) redox probe at a scan rate of 80 mV s^{-1} . The experimentally recorded currents have been normalised against the analyte concentration. Although the results for the 2% CH_4/H_2 electrode are comparable to that found for the 0.5% material, a notable difference is the significant decrease in the recorded peak-to-peak separation. For example the peak-to-peak separation of the 0.5% CH_4/H_2 electrode at the concentration level of 0.5 mM is 170 mV. In comparison with the 2.0% material, the peak-to-peak separation decreased to 120 mV.

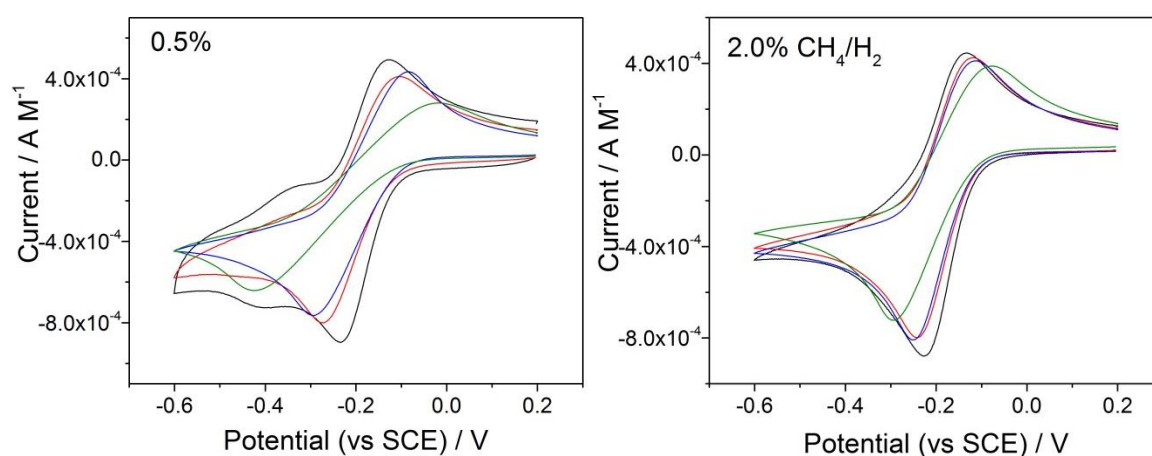


Fig. 6: Normalized CV voltammograms for the original concentration of $\text{Ru}(\text{NH}_3)_6^{3+/2+}$: 0.1 mM (black), 0.5 mM (red), 1 mM (blue) and 3 mM (green) using electrodes with 0.5 % and 2.0 % CH_4/H_2 ratio, scan rate 80 mV s^{-1} .

This decrease in the peak-to-peak separation in the voltammetric response for the 2% CH_4/H_2 electrodes implies that the resistivity of the electrodes is less than that of the 0.5% CH_4/H_2 material. Note that due to the use of ruthenium(III) hexamine as the redox probe it is highly unlikely that the alteration of the voltammetric response relates to a change in the apparent electron transfer kinetics because the rate constant should be largely independent of the electrode surface nature [7].

3.3 Reconciling the electrochemical and physical data

The low boron-doped thin-film diamond electrodes presented in the work exhibit distinct electrochemical activity and importantly the behaviour of the material produced with 2% CH₄/H₂ exhibits a more ‘ideal’ voltammetric response, in that the electrochemical peak-to-peak separation is smaller and the voltammetry appears to be less sensitive to the concentration of the analyte. We suggest that the electrochemical activity is ultimately dominated by the presence of non-diamond impurities. Were the electrodes behaving in a manner expected of a semi-conducting material the redox response of ruthenium would not be expected to be observable and the electrode should exhibit diode like behaviour. Problematically at first sight from analysis of the relative magnitudes of the G and D peak heights in the Raman spectra it is concluded that the qualitative graphitic carbon content in the 2% CH₄/H₂ is in fact *less* than that found for the material grown in a lower methane concentration (0.5%). However, in all cases the Raman spectroscopy does evidence the significant presence of non-diamond carbon. Recognising that the difference in the electrochemical behaviour cannot be sufficiently explained by the magnitude of the peaks in the Raman spectra we turn to consider the influence of the electrode morphology. First, as shown in the SEM images (Fig. 1), the grain size for the HFCVD thin-film diamond varies from an average dimension of 141±49 nm to 485±128 nm as the ratio of CH₄/H₂ changes from 0.5% to 2.0%. Hence, in all cases the crystalline diamond is sub-micron in scale. Second, any graphitic (sp²) or other non-diamond impurities will be present at the grain boundaries [17]. Due to the dimensions of the grains being *relatively* small compared to the distance diffused by the ruthenium(III) hexamine over the course of the voltammetric experiment (65 - 260 μm as approximated via the Einstein equation, $d \sim (2Dt)^{0.5}$) the diffusion layers associated with individual grain boundaries will strongly overlap. Hence, given the increase in the diamond grain size and the only relatively small decrease in the sp²/sp³ Raman spectroscopy ratio, it is concluded that concomitant with the alteration in the

diamond grain size the dimensions of the graphitic impurity domains at the grain boundaries are likely altered. Hence, it is notable that the change in the morphology and increase in the dimensions of the sp^2 and other non-diamond carbon impurity domains leads to a lowering of the effective resistance of the thin-film diamond. This local lowering of the films resistivity gives rise to the relatively more ‘ideal’ voltammetric responses recorded for the 2% CH_4/H_2 HFCVD non-boron doped diamond thin-films.

4. Conclusions

This work provides an example case highlighting the limitations of the use of Raman spectroscopy for the characterisation of low doped diamond based electrodes. Specifically, due to diffusional overlap the voltammetric response of an electrode can be dominated by a minority of active sites. This work further highlights the importance of the morphology of the non-diamond electrode impurities. It is found that the produced electrodes with larger grain sizes but marginally lower sp^2/sp^3 ratios (as evidenced via Raman spectroscopy) yield voltammetric response which are relatively more ‘ideal’ i.e. they exhibit smaller peak-to-peak separations. First, the direct use of the qualitative information about sp^2 and sp^3 bonded carbon content as obtained from Raman spectroscopy is cautioned when seeking insight into the electrochemical behaviour of an electrode. Second, for diamond electrodes with sub-micron scale heterogeneity it is demonstrated how the inherent activity of the electrode – even in the absence of high levels of boron doping – may be very significant. Consequently, it is unlikely that significant physical insight into the activity of similar diamond electrodes even with higher boron contents can be made simply through consideration of their dopant concentration.

5. Acknowledgements

This work was supported by the Grant Agency of the Slovak Republic (Grant No. 1/0489/16), Grant scheme for Support of Young Researchers and Excellent Teams of Young Researchers and the Slovak Research and Development Agency (APVV-0365-12). KC acknowledges financial support by the National Scholarship Programme of the Slovak Republic and Tatrabanka Foundation for supporting her research stay in Oxford.

References

- [1] R. G. Compton, J. S. Foord, F. Marken, Electroanalysis at diamond-like and doped-diamond electrodes, *Electroanal.*, 15 (2003) 1349-1363.
- [2] Y. V. Pleskov, Electrochemistry of diamond: A review, *Russ. J. Electrochem.*, 38 (2002) 1275-1291.
- [3] Y. Einaga, J.S. Foord, G.M. Swain, Diamond electrodes: Diversity and maturity, *MRS Bull.*, 39 (2014) 525-532.
- [4] N. Yang, J.S. Foord, X. Jiang, Diamond electrochemistry at the nanoscale, *Carbon*, 99 (2016) 90-110.
- [5] H. Randriamahazaka, J. Ghilane, Electrografting and controlled surface functionalization of carbon based surfaces for electroanalysis, *Electroanal.*, 28 (2016) 13-26.
- [6] M.M. Barsan, C.M.A. Brett, Recent advances in layer-by-layer strategies for biosensors incorporating metal nanoparticles, *TrAC*, 79 (2016) 286-296.
- [7] K. B. Holt, A. J. Bard, Y. Show, G.M. Swain, Scanning electrochemical microscopy and conductive probe atomic force microscopy studies of hydrogen-terminated boron-doped diamond electrodes with different doping levels, *J. Phys. Chem. B*, 108 (2004) 15117-15127.
- [8] C.H. Goeting, F. Marken, A. Gutiérrez-Sosa, R.G. Compton, J.S. Foord, Electrochemically induced surface modifications of boron-doped diamond electrodes: an X-ray photoelectron spectroscopy study, *Diam. Relat. Mater.*, 9 (2000) 390-396.

- [9] J.V. Macpherson, A practical guide to using boron doped diamond in electrochemical research, *Phys. Chem. Chem. Phys.*, 17 (2015) 2935-2949.
- [10] V. Chakrapani, J.C. Angus, A.B. Anderson, S.D. Wolter, B.R. Stoner, G.U. Sumanasekera, Charge transfer equilibria between diamond and an aqueous oxygen electrochemical redox couple, *Science*, 318 (2007) 1424-1430.
- [11] S. Garcia-Segura, E. Vieira dos Santos, C.A. Martínez-Huitle, Role of sp^3/sp^2 ratio on the electrocatalytic properties of boron-doped diamond electrodes: a mini review, *Electrochem. Commun.*, 59 (2015) 52-55.
- [12] K. Fabisiak, M. Kowalska, M. Szybowicz, K. Paprocki, P. Popielarski, A. Wrzyszczyński et al., The undoped CVD diamond electrode: the effect of surface pretreatment on its electrochemical properties, *Adv. Eng. Mater.*, 15 (2013) 935-940.
- [13] S. Wang, G.M. Swain, Spatially heterogeneous electrical and electrochemical properties of hydrogen-terminated boron-doped nanocrystalline diamond thin film deposited from an argon-rich $CH_4/H_2/Ar/B_2H_6$ source gas mixture, *J. Phys. Chem. C*, 111 (2007) 3986-3995.
- [14] F. Maier, M. Riedel, B. Mantel, J. Ristein, L. Ley, Origin of surface conductivity in diamond, *Phys. Rev. Lett.*, 85, (2000) 3472-3475.
- [15] C.E. Nebel, B. Rezek, D. Shin, H. Watanabe, Surface electronic properties of H-terminated diamond in contact with adsorbates and electrolytes, *Phys. Status Solidi A*, 203 (2006) 203, 3273-3298.
- [16] C.E. Nebel, H. Kato, B. Rezek, D. Shin, D. Takeuchi, H. Watanabe, et al., Electrochemical properties of undoped hydrogen terminated CVD diamond, *Diam. Relat. Mater.*, 15 (2006) 264-268.
- [17] K.B. Holt, Ch. Ziegler, J. Zang, J. Hu, J.S. Foord, Scanning electrochemical microscopy studies of redox processes at undoped nanodiamond surfaces, *J. Phys. Chem. C*, 113 (2009) 2761-2770.

- [18] J. Foord, J.P. Hu, Electrochemical oxidation and reduction processes at diamond electrodes of varying phase purity, *Phys. Status Solidi A*, 203 (2006) 3121-3127.
- [19] Y.V. Pleskov, M.D. Krotova, V.G. Ralchenko, A.V. Khomich, R.A. Khmelnitskiy, Vacuum-annealed undoped polycrystalline CVD diamond: a new electrode material, *Electrochim. Acta*, 49 (2003) 41-49.
- [20] R. Kinder, M. Mikolášek, D. Donoval, J. Kováč, M. Tlaczala, Measurement system with hall and four point probes for characterization of semiconductors, *J. Electr. Eng.*, 64 (2013) 106-111.
- [21] O.V. Klymenko, R.G. Evans, Ch. Hardacre, I.B. Svir, R.G. Compton, Double potential step chronoamperometry at microdisk electrodes: simulating the case of unequal diffusion coefficients, *J. Electroanal. Chem.*, 571 (2004) 211-221.
- [22] D.S. Knight, W.B. White, Characterization of diamond films by Raman spectroscopy, *J. Mater. Res.*, 4 (1989) 385-393.
- [23] A.C. Ferrari, J. Robertson, Origin of the $1,150\text{ cm}^{-1}$ Raman mode in nanocrystalline diamond, *Phys. Rev. B*, 63 (2001) 121405.
- [24] T.W. Hamann, F. Gstrein, B. S. Brunshwig, N.S. Lewis, Measurement of the free-energy dependence of interfacial charge-transfer rate constants using $\text{ZnO}/\text{H}_2\text{O}$ semiconductor/liquid contacts, *J. Am. Chem. Soc.* 127 (2005) 7815-7824.
- [25] A.J. Bard, L.R. Faulkner, *Electrochemical methods: fundamentals and applications*, Wiley, New York, 1980.
- [26] E.J.F. Dickinson, J.G. Limon-Petersen, N.V. Rees, R.G. Compton, How much supporting electrolyte is required to make a cyclic voltammetry experiment quantitatively "diffusional"? A theoretical and experimental investigation, *J. Phys. Chem. C*, 113 (2009) 11157-11171.

- [27] T.J. Davies, C.E. Banks, R.G. Compton, Voltammetry at spatially heterogeneous electrodes, *J. Solid State Electrochem.*, 9 (2005) 797-808.
- [28] T.J. Davies, S. Ward-Jones, C.E. Banks, J. del Campo, R. Mas, et al., The cyclic and linear sweep voltammetry of regular arrays of microdisc electrodes: fitting of experimental data, *J. Electroanal. Chem.*, 585 (2005) 51-62.